PCCP

COMMUNICATION

Alpha-tocopherol inhibits pore formation in oxidized bilayers†

Phansiri Boonnoy,[ab] Mikko Karttunen[cd] and Jirasak Wong-ekkabut*[abe]

Cite this: *Phys. Chem. Chem. Phys.*, 2017, **19**, 5699

Received 24th November 2016,
Accepted 24th January 2017

DOI: 10.1039/c6cp08051k

rsc.li/pccp

In biological membranes, alpha-tocopherols (α-toc; vitamin E) protect polyunsaturated lipids from free radicals. Although the interactions of α-toc with non-oxidized lipid bilayers have been studied, their effects on oxidized bilayers remain unknown. In this study, atomistic molecular dynamics (MD) simulations of oxidized lipid bilayers were performed with varying concentrations of α-toc. Bilayers with 1-palmitoyl-2-lauroyl-*sn*-glycero-3-phosphocholine (PLPC) lipids and their aldehyde derivatives at a 1:1 ratio were studied. Our simulations show that oxidized lipids self-assemble into aggregates with a water pore rapidly developing across the bilayer. The free energy of transporting an α-toc molecule in a bilayer suggests that α-tocs can passively adsorb into it. When α-toc molecules were present at low concentrations in bilayers containing oxidized lipids, water pore formation was slowed down. At high α-toc concentrations, no pores were observed. Based on the simulations, we propose that the mechanism of how α-toc inhibits pore formation in bilayers with oxidized lipids is the following: α-tocs trap the polar groups of the oxidized lipids at the membrane–water interface resulting in a decreased probability of the oxidized lipids making contact with the two leaflets and initiating pore formation. This demonstrates that α-toc molecules not only protect the bilayer from oxidation but also help to stabilize the bilayer after lipid peroxidation occurs. These results will help in designing more efficient molecules to protect membranes from oxidative stress.

Biological membranes serve as a partition between cells and their environment. Under oxidative stress, unsaturated lipids present in cell membranes may become exposed to attacks by free radicals, that is, oxidation. Oxidation transforms some of the membrane lipids to oxidized ones such as hydroperoxide and aldehyde lipids.[1,2] It has also been suggested that internal, that is intra-leaflet, oxidation may be important in altering bilayer properties.[3]

Lipid peroxidation is an important mechanism of cell membrane damage.[4–6] Previous experiments and computer simulations[4,7–14] have demonstrated how oxidized lipids disturb and deform bilayers. The retention of the polar chains of oxidized lipids in the bilayer's interior is energetically unfavorable resulting in the reversal of the polar lipid chain to the bilayer interface.[4,11,15,16] This reversal causes major changes in bilayer properties such as an increase in area per lipid, bilayer thinning, decrease of the lipid tail order parameter, and increase in water permeability.[4,12,15–18] Previously, we performed MD simulations of lipid bilayers with oxidized lipids at high concentrations. Two major oxidized lipid species, hydroperoxide and aldehyde, were studied. The results showed that only aldehyde lipids were able to induce pore formation across a PLPC bilayer and cause significant deformation.[13,15]

α-toc is well-known as an efficient antioxidant that protects membranes from free radical-initiated oxidation.[19–21] Natural membranes consist of saturated and unsaturated lipids, and they are permeable to water and small molecules. Unsaturated lipids play an important role in membrane permeability by disrupting the packing of saturated lipids. However, unsaturated lipids are readily susceptible to peroxidation which, if extreme, may lead to uncontrollable transport of molecules across the membrane.[22] Numerous studies have been conducted to find the mechanisms of how α-toc protects polyunsaturated fatty acids from free radicals and to explain how α-toc interacts with biological membranes.[21,23–28] Protective mechanisms in the absence of oxidized lipids have been proposed, for example that the chromanol group of the α-toc molecule can bind and trap free radicals within the interior and near the membrane interface[26] thus blocking their ability to enter the membrane and oxidize polyunsaturated lipid chains.

In previous studies, interactions of α-toc have been considered with non-oxidized lipid bilayers only[24–28] and the effects of α-toc on bilayers with oxidized lipids remain unresolved. To understand how α-tocs interact with biological membranes after lipid peroxidation,

[a] *Department of Physics, Faculty of Science, Kasetsart University, Bangkok 10900, Thailand. E-mail: jirasak.w@ku.ac.th*
[b] *Computational Biomodelling Laboratory for Agricultural Science and Technology (CBLAST), Faculty of Science, Kasetsart University, Bangkok 10900, Thailand*
[c] *Department of Mathematics and Computer Science & Institute for Complex Molecular Systems, Eindhoven University of Technology, MetaForum, 5600 MB Eindhoven, The Netherlands*
[d] *Departments of Chemistry and Applied Mathematics, Western University, 1151 Richmond Street, London, Ontario N6A 5B7, Canada*
[e] *Thailand Center of Excellence in Physics (ThEP Center), Commission on Higher Education, Bangkok 10400, Thailand*

† Electronic supplementary information (ESI) available. See DOI: 10.1039/c6cp08051k

MD simulations of α-toc in oxidized lipid bilayers were carried out. Previous studies[13,15] without α-toc have shown that the presence of aldehyde lipids could lead to large disturbances of the bilayer. Water defects have been experimentally observed at 12.5–20 mol% of oxidation in 1-palmitoyl-2-oleoyl-*sn-glycero*-3-phosphocholine (POPC) membranes.[18,29] In a computational study,[17] water pore formation in the 1,2-dioleoyl-*sn-glycero*-3-phosphocholine (DOPC) bilayer was observed at high oxidation (75–100 mol%). Recently, our simulations[13] with significantly longer simulation times (microseconds) suggested that the pore formation in oxidized PLPC bilayers was unlikely to occur at aldehyde concentrations below 50%. To achieve pore formation within reasonable computational time, 1 : 1 binary lipid bilayer mixtures between PLPC and its two aldehyde lipids 1-palmitoyl-2-(9-oxo-nonanoyl)-*sn-glycero*-3-phosphocholine (9-al) and 1-stearoyl-2-(12-oxo-*cis*-9-dodecenoyl)-*sn-glycero*-3-phosphocholine (12-al) were chosen for this study. The molecular structures are shown in Fig. S1 (ESI†).

Methods

The simulated systems consisted of 0–16 α-toc molecules embedded in lipid bilayers with 128 phospholipid molecules and 10 628 simple point charge (SPC)[30] water molecules. All the simulated systems are listed in Table 1. Repeated simulations for each system were performed to verify reproducibility of the results. The topologies and force field parameters of α-toc were taken from Qin *et al.*[24,25] The lipid parameters were taken from previous studies.[4,13,31] Initially, the α-toc molecules were randomly placed in the water phase about 4.2 nm away from the center of mass (COM) of the bilayer. After energy minimization, MD simulations were run for 1–2 μs with a 2 fs integration time step by using the GROMACS 4.5.5 package.[32,33] Periodic boundary conditions were applied in all directions. The neighbor list was updated at every time step. A cutoff was employed at 1.0 nm for the real space part of electrostatic interactions and Lennard-Jones interactions. The Ewald particle-mesh[34–36] was used to calculate the long-range part of electrostatic interactions and all bond lengths were constrained by the LINCS algorithm.[37] In all simulations, the temperature was set to 298 K using the v-rescale algorithm[38] with a time constant of 0.1 ps. Pressure was controlled by the Parrinello–Rahman algorithm[39,40] with an equilibrium semi-isotropic pressure of 1 bar, a time constant of 4.0 ps and compressibility of 4.5×10^{-5} bar^{-1}. These parameters and protocols have been extensively tested and optimized.[41–43] All visualizations were carried out using Visual Molecular Dynamic (VMD) software.[44]

Free energy calculations

The potential of mean force (PMF) of an α-toc transferring into the lipid bilayer was calculated using the umbrella sampling technique[45] with the Weighted Histogram Analysis Method[46] (WHAM). Three bilayers of 100% PLPC, 50% 12-al, and 50% 9-al were used. A series of 41 simulations was run with the distance between α-toc and the bilayer center restrained between 0 and 4.0 nm, with 0.1 nm spacing. In the first window, the α-toc molecule is in bulk water. It was then subsequently moved into the bilayer along the bilayer normal (*z*-axis) in each successive window. Therefore, the final window had the α-toc molecule at the bilayer center. The hydroxyl of α-toc was restrained with respect to the center of mass of the bilayer, using a harmonic restraint with a force constant of 3000 kJ $(mol\ nm^2)^{-1}$ normal to the bilayer. Simulations were performed in the NPT ensemble at 298 K for a total time of 2.05 μs. Each window was run at least for 50 ns and the last 20 ns was used for analysis. The bootstrap analysis method[47] was used to estimate the statistical uncertainty in umbrella sampling simulations.

Results

The MD simulations show that without α-toc, oxidized lipids self-assemble to form aggregates and a water pore develops rapidly across the bilayer (Fig. 1). A pore spanning the bilayer occurred afterward. This result is in agreement with previous studies.[13] At low α-toc concentrations (2 and 4 α-toc molecules in a bilayer), the α-toc molecules' preferred position was close to the bilayer interface which lead to slowed down formation (as compared with no α-toc present) of a water pore over several hundreds of nanoseconds, Table 1. Interestingly, when the α-toc

Table 1 Compositions of α-toc in the different oxidized lipid bilayers used in this study

No.	System name	Proportion	Final structure	Pore time (ns)
1	100% PLPC	128 PLPC	Bilayer	—
2	100% PLPC + 1 α-toc	128 PLPC : 1 α-toc	Bilayer	—
3	50% 12-al	64 PLPC : 64 12-al	Bilayer with a pore	140, 238
4	50% 12-al + 2 α-toc	64 PLPC : 64 12-al : 2 α-toc	Bilayer with a pore	337, 1100
5	50% 12-al + 4 α-toc	64 PLPC : 64 12-al : 4 α-toc	Bilayer with a pore	340, 266
6	50% 12-al + 8 α-toc	64 PLPC : 64 12-al : 8 α-toc	Bilayer	—
7	50% 12-al + 16 α-toc	64 PLPC : 64 12-al : 16 α-toc	Bilayer	—
8	50% 9-al	64 PLPC : 64 9-al	Bilayer with a pore	180, 50
9	50% 9-al + 2 α-toc	64 PLPC : 64 9-al : 2 α-toc	Bilayer with a pore	212, 100
10	50% 9-al + 4 α-toc	64 PLPC : 64 9-al : 4 α-toc	Bilayer with a pore	809, 620
11	50% 9-al + 8 α-toc	64 PLPC : 64 9-al : 8 α-toc	Bilayer	—
12	50% 9-al + 16 α-toc	64 PLPC : 64 9-al : 16 α-toc	Bilayer	—

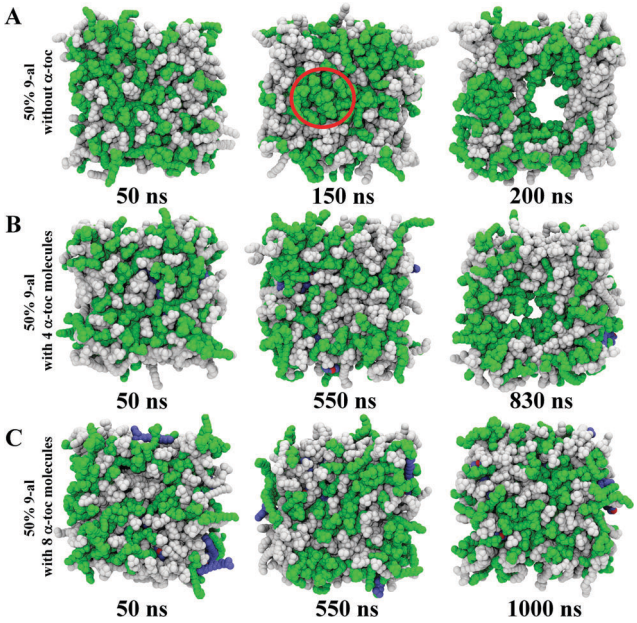

Fig. 1 Time evolution of a 50% 9-al lipid bilayer (A) without α-toc, (B) with 4 α-toc molecules, and (C) with 8 α-toc molecules. Water molecules are not shown for clarity. White, green, purple: PLPC, 9-al and α-toc molecules, respectively. Red: oxygen atoms of the α-toc hydroxyl groups. The red circle represents the oxidized lipids' aggregation region.

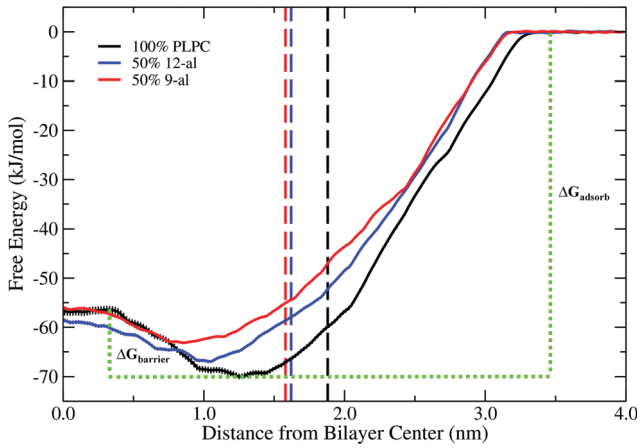

Fig. 3 The potential of mean force (PMF) of an α-toc transferring into the bilayer as a function of distance in the z-direction from the center of the bilayer (z = 0.0 nm). The curves show bilayers of 100% PLPC, 50% 12-al and 50% 9-al in black, blue, and red lines, respectively. Bulk water defines zero free energy. The dashed lines represent the average position of P atoms in each bilayer. The free energies of α-toc adsorbing in the 100% PLPC, 50% 12-al, and 50% 9-al bilayer are −70.0, −67.0, and −63.2 kJ mol^{-1}, respectively. The free energy barriers of α-toc in the 100% PLPC, 50% 12-al, and 50% 9-al bilayers are 13.6, 8.4, and 7.1 kJ mol^{-1}, respectively. The maximum statistical uncertainties of 100% PLPC, 50% 12-al, and 50% 9-al are 0.8, 0.4, and 0.3 kJ mol^{-1}, respectively.

concentration was increased, no pore formation was observed over the entire simulation time of over 2 μs.

Fig. 2 shows (unbiased MD simulation) that α-toc is able to passively penetrate into the bilayer and remain in the bilayer interior around the carbonyl groups of the lipids. In agreement with free energy calculations (Fig. 3), it is energetically favorable for α-toc to enter the bilayer. The free energy calculation shows that the adsorption energy of α-toc into a PLPC bilayer is −70.0 kJ mol^{-1} with the equilibrium position being about 1.3 nm from the center of the bilayer. For moving the α-toc from equilibrium toward the center of the bilayer, an energy barrier with a steep slope and magnitude of 13.6 kJ mol^{-1} was observed (Fig. 3). After reaching the maximum of the free energy barrier, the PMF plateaus at

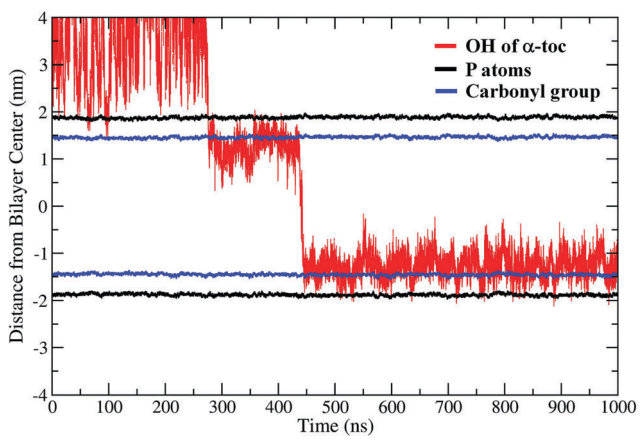

Fig. 2 The time evolution of the position of the hydroxyl group of an α-toc molecule in the 100% PLPC bilayer.

−56.8 kJ mol^{-1}. Our PMF profile is qualitatively similar to that of a cholesterol molecule transferring from water into a DPPC lipid bilayer.[48] As a comparison, the free energies of cholesterol transferring from water in DPPC lipid bilayers to the center of the bilayer and equilibrium are −50 and −67 kJ mol^{-1}, respectively.[48] This result suggests that it is more favorable for an α-toc molecule to stay in lipid bilayer than cholesterol. Note that some of the quantitative differences might come from other parameters such as the type of lipid and temperature, and thus further studies are needed to establish the differences more accurately.[48]

The free energy barrier of an α-toc between equilibrium and the bilayer's center was 13.6 kJ mol^{-1} (Fig. 3) and as a result, flip-flop of an α-toc in the pure PLPC bilayer was observed only once. The PMF profiles of α-toc in oxidized bilayers are qualitatively similar to a non-oxidized bilayer but the adsorption energies were increased to −67.0 and −63.2 kJ mol^{-1} in 50% 12-al and 50% 9-al bilayers, respectively. The equilibrium positions of the α-tocs were deep inside the bilayer consistent with a decrease in the thickness of the bilayer. These results suggest that α-toc molecules prefer to interact with non-oxidized lipids and stay inside the non-oxidized bilayer as compared to the oxidized system. Moreover, the free energy barriers from equilibrium toward the center of the bilayer of 50% 12-al and 50% 9-al were 8.4 and 7.1 kJ mol^{-1}, respectively. The observed decrease of the free energy barriers in oxidized bilayers results in frequent flip-flops of α-toc (Fig. 4). Moreover, α-tocs always formed hydrogen bonds with the aldehyde groups of the oxidized lipids' tails. Flip-flops of α-tocs occurred when such hydrogen bonds were lost and re-formed with aldehyde groups in the opposite leaflet as shown in Fig. 4 and Fig. S2 (ESI†). In membranes containing no oxidized lipids, α-toc flip-flops have previously been observed only at the temperature of 350 K but

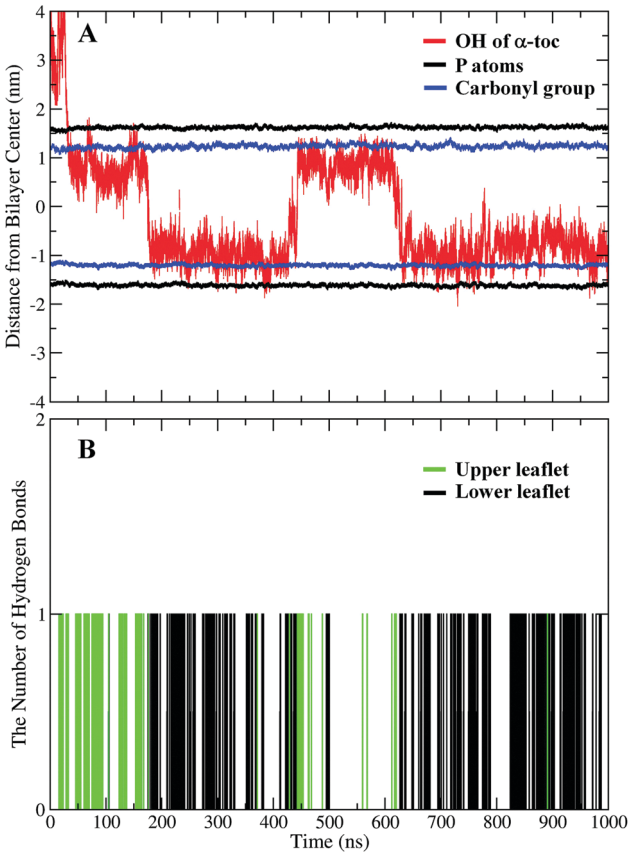

Fig. 4 (A) The time evolution of the position of the hydroxyl group of α-toc from the center of the 50% 9-al lipid bilayer (along the *z*-axis). (B) The number of hydrogen bonds between the hydroxyl groups of α-tocs and the aldehyde groups of the oxidized lipid tails in the upper and lower leaflets. This result is from only one of eight α-toc molecules in the system of 50% 9-al with 8 α-toc and the rest of the α-toc molecules are shown in Fig. S2 (ESI†).

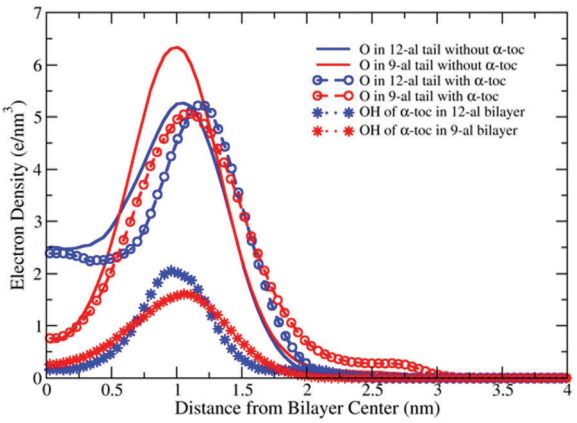

Fig. 5 Electron density profiles for the oxygen atoms in the oxidized lipid hydrocarbon chains with and without α-toc, and for the hydroxyl groups of α-toc in 50% 12-al and 50% 9-al bilayers. The bilayers with α-toc consisted of 16 α-toc molecules.

not below.[24] These results suggest that α-toc is highly mobile inside bilayers containing oxidized lipids.

Electron density distributions (Fig. 5) show that the hydroxyl groups of α-toc molecules have their maxima at 0.96 nm and 1.06 nm for the 50% 12-al and 50% 9-al systems, respectively. These maxima are related to the locations of the carbonyl groups of the lipid bilayers and are consistent with Fig. 4 and previous studies.[24,26–28] Surprisingly, the electron density of the oxygen atoms in oxidized lipids' tails decreased at the bilayer's center and increased at the water interface when α-toc molecules were present. Our previous study suggested that one of the key mechanisms for passive pore formation is the distribution of polar groups inside the bilayer.[13] The deep penetration of the polar group inside the bilayer can bring lipids into contact with lipids in the opposite leaflet thus leading to the formation of a water bridge and consequently a stable pore.

When α-tocs are present in a bilayer, they are able to trap the polar groups of the oxidized lipids at the water interface (Fig. 4 and 5) resulting in a decreased probability of the oxidized lipids being in contact with each other. Therefore, pores cannot be formed at high α-toc concentrations. Furthermore, water transport across lipid bilayers with non-oxidized lipids is not frequent, since the free energy barrier of a water molecule crossing a PLPC bilayer is 29.4 ± 2.3 kJ mol^{-1}.[4] Permeability also increases by an order of magnitude as the concentration of oxidized lipids increases.[17,18] Moreover, permeability increases by three orders of magnitude when a pore spans the bilayer (Table 2, Fig. S3, ESI†). When the concentration of α-toc inside the bilayer increases, water permeability decreases and pore formation becomes inhibited (Table 2).

The deuterium order parameter for the *sn-1* chain of PLPC and oxidized lipids (Fig. S4, ESI†) shows that all systems of lipid bilayers are in the biologically relevant liquid crystalline phase and the order parameter increases with increasing α-toc concentration. Cholesterol and α-toc molecules have similar molecular structures consisting of a hydrophobic tail and a ring-structure with a hydroxyl group. The effects of these molecules on biological membranes are similar and this has been suggested to be responsible for the observed increase in bilayer thickness and lipid tail order.[25,49,50] Moreover, Issack *et al.*[51] have shown that

Table 2 Water permeability through the oxidized lipid bilayer

No.	System name	Bilayer Permeability (p_f) cm^3 s^{-1} ($\times 10^{-15}$)	Pore Permeability (p_f) cm^3 s^{-1} ($\times 10^{-12}$)
1	100% PLPC	0.96 ± 0.24	—
2	100% PLPC + 1 α-toc	0.44 ± 0.16	—
3	50% 12-al	6.00 ± 1.94	7.31 ± 0.31
4	50% 12-al + 2 α-toc	3.27 ± 0.59	4.72 ± 0.59
5	50% 12-al + 4 α-toc	3.61 ± 0.85	5.89 ± 0.40
6	50% 12-al + 8 α-toc	4.22 ± 0.53	—
7	50% 12-al + 16 α-toc	2.81 ± 0.45	—
8	50% 9-al	4.50 ± 1.65	8.97 ± 0.34
9	50% 9-al + 2 α-toc	3.72 ± 0.87	8.28 ± 0.43
10	50% 9-al + 4 α-toc	3.55 ± 0.53	6.06 ± 1.47
11	50% 9-al + 8 α-toc	2.21 ± 0.48	—
12	50% 9-al + 16 α-toc	2.57 ± 0.45	—

Note: Water permeability was calculated using $p_f = \nu_w R_t/NA$, where ν_w is the average volume of a single water molecule, 18 cm^3 mol^{-1}, R_t is the rate of water transport across the bilayer and NA is Avogadro's number.

the free-energy barrier for transferring a water molecule to the center of the bilayer was increased by 6 kJ mol^{-1} when 41 mol% cholesterol was present in a DPPC bilayer. This observed significant increase in the free energy barrier to transfer water through the bilayer with the presence of cholesterol results in a decrease in water permeability.[51,52]

In conclusion, free radicals play an important role in membrane damage and aldehyde lipids are the major oxidative lipid product that causes pore formation and bilayer deformation.[13,19–21] On the other hand, α-toc is one of the most effective antioxidants in removing free radicals and it has been used in cosmetics, functional foods and many other applications.[53–55] Previously,[19–21,26] the only protective mechanism of α-toc against lipid peroxidation in biological membranes was proposed to be due to α-toc blocking free radicals' entry into the membrane thus protecting polyunsaturated lipid chains from oxidation processes, that is, with no oxidized lipids in the bilayer. In a realistic case, however, oxidized lipids are present and it is important to understand how their destructive effects can be prevented. In this study, we have shown that α-toc molecules can inhibit pore formation in oxidized lipid bilayers by confining the polar groups of the oxidized lipids at the water interface. Our findings also suggest that by controlling α-toc concentration, the stability of biological membranes can be increased. This understanding of how α-tocs affect oxidized membranes is likely to be beneficial for designing new molecules to protect, *e.g.*, skin, against aging[56,57] and in plasma treatment of cancer.[49]

Competing financial interests

The authors declare no competing financial interest.

Acknowledgements

Financial support by Kasetsart University Research & Development Institute (KURDI; J. W.) and Faculty of Science (J. W.) is acknowledged.

References

1 T. K. Mandal and S. N. Chatterjee, *Radiat. Res.*, 1980, **83**, 290–302.
2 S. N. Chatterjee and S. Agarwal, *Free Radical Biol. Med.*, 1988, **4**, 51–72.
3 P. L. Else and E. Kraffe, *Biochim. Biophys. Acta*, 2015, **1848**, 417–421.
4 J. Wong-ekkabut, Z. Xu, W. Triampo, I. M. Tang, D. Peter Tieleman and L. Monticelli, *Biophys. J.*, 2007, **93**, 4225–4236.
5 H. Y. Yin, L. B. Xu and N. A. Porter, *Chem. Rev.*, 2011, **111**, 5944–5972.
6 E. Niki, Y. Yoshida, Y. Saito and N. Noguchi, *Biochem. Biophys. Res. Commun.*, 2005, **338**, 668–676.
7 X. M. Li, R. G. Salomon, J. Qin and S. L. Hazen, *Biochemistry*, 2007, **46**, 5009–5017.
8 J. P. Mattila, K. Sabatini and P. K. Kinnunen, *Langmuir*, 2008, **24**, 4157–4160.
9 K. Sabatini, J. P. Mattila, F. M. Megli and P. K. Kinnunen, *Biophys. J.*, 2006, **90**, 4488–4499.
10 L. Beranova, L. Cwiklik, P. Jurkiewicz, M. Hof and P. Jungwirth, *Langmuir*, 2010, **26**, 6140–6144.
11 H. Khandelia and O. G. Mouritsen, *Biophys. J.*, 2009, **96**, 2734–2743.
12 V. Jarerattanachat, M. Karttunen and J. Wong-ekkabut, *J. Phys. Chem. B*, 2013, **117**, 8490–8501.
13 P. Boonnoy, V. Jarerattanachat, M. Karttunen and J. Wong-ekkabut, *J. Phys. Chem. Lett.*, 2015, **6**, 4884–4888.
14 P. Siani, R. M. de Souza, L. G. Dias, R. Itri and H. Khandelia, *Biochim. Biophys. Acta*, 2016, **1858**, 2498–2511.
15 L. Cwiklik and P. Jungwirth, *Chem. Phys. Lett.*, 2010, **486**, 99–103.
16 J. Garrec, A. Monari, X. Assfed, L. M. Mir and M. Tarek, *J. Phys. Chem. Lett.*, 2014, **5**, 1653–1658.
17 M. Lis, A. Wizert, M. Przybylo, M. Langner, J. Swiatek, P. Jungwirth and L. Cwiklik, *Phys. Chem. Chem. Phys.*, 2011, **13**, 17555–17563.
18 K. A. Runas and N. Malmstadt, *Soft Matter*, 2015, **11**, 499–505.
19 E. Niki and M. G. Traber, *Ann. Nutr. Metab.*, 2012, **61**, 207–212.
20 X. Wang and P. J. Quinn, *Prog. Lipid Res.*, 1999, **38**, 309–336.
21 M. G. Traber and J. Atkinson, *Free Radical Biol. Med.*, 2007, **43**, 4–15.
22 M. H. Brodnitz, *J. Agric. Food Chem.*, 1968, **16**, 994–999.
23 V. E. Kagan, *Ann. N. Y. Acad. Sci.*, 1989, **570**, 121–135.
24 S. S. Qin, Z. W. Yu and Y. X. Yu, *J. Phys. Chem. B*, 2009, **113**, 16537–16546.
25 S. S. Qin and Z. W. Yu, *Acta Phys.-Chim. Sin.*, 2011, **27**, 213–227.
26 X. L. Leng, J. J. Kinnun, D. Marquardt, M. Ghefli, N. Kucerka, J. Katsaras, J. Atkinson, T. A. Harroun, S. E. Feller and S. R. Wassall, *Biophys. J.*, 2015, **109**, 1608–1618.
27 D. Marquardt, N. Kučerka, J. Katsaras and T. A. Harroun, *Langmuir*, 2014, **31**, 4464–4472.
28 D. Marquardt, J. A. Williams, N. Kucerka, J. Atkinson, S. R. Wassall, J. Katsaras and T. A. Harroun, *J. Am. Chem. Soc.*, 2013, **135**, 7523–7533.
29 R. Volinsky, L. Cwiklik, P. Jurkiewicz, M. Hof, P. Jungwirth and P. K. Kinnunen, *Biophys. J.*, 2011, **101**, 1376–1384.
30 H. J. C. Berendsen, J. P. M. Postma, W. F. van Gunsteren and J. Hermans, in *Intermol. Forces*, ed. B. Pullman, D. Reidel, Dordrecht, The Netherlands, 1981, pp. 331–342.
31 M. Bachar, P. Brunelle, D. P. Tieleman and A. Rauk, *J. Phys. Chem. B*, 2004, **108**, 7170–7179.
32 B. Hess, C. Kutzner, D. van der Spoel and E. Lindahl, *J. Chem. Theory Comput.*, 2008, **4**, 435–447.
33 S. Pronk, S. Pall, R. Schulz, P. Larsson, P. Bjelkmar, R. Apostolov, M. R. Shirts, J. C. Smith, P. M. Kasson, D. van der Spoel, B. Hess and E. Lindahl, *Bioinformatics*, 2013, **29**, 845.
34 T. Darden, D. York and L. Pedersen, *J. Chem. Phys.*, 1993, **98**, 10089–10092.
35 U. Essmann, L. Perera, M. L. Berkowitz, T. Darden, H. Lee and L. G. Pedersen, *J. Chem. Phys.*, 1995, **103**, 8577–8593.

36 M. Karttunen, J. Rottler, I. Vattulainen and C. Sagui, *Curr. Top. Membr.*, 2008, **60**, 49.
37 B. Hess, H. Bekker, H. J. C. Berendsen and J. G. E. M. Fraaije, *J. Comput. Chem.*, 1997, **18**, 1463–1472.
38 G. Bussi, D. Donadio and M. Parrinello, *J. Chem. Phys.*, 2007, **126**, 014101.
39 M. Parrinello and A. Rahman, *J. Appl. Phys.*, 1981, **52**, 7182–7190.
40 S. Nosé and M. L. Klein, *Mol. Phys.*, 1983, **50**, 1055–1076.
41 J. Wong-Ekkabut, M. S. Miettinen, C. Dias and M. Karttunen, *Nat. Nanotechnol.*, 2010, **5**, 555–557.
42 J. Wong-ekkabut and M. Karttunen, *J. Chem. Theory Comput.*, 2012, **8**, 2905–2911.
43 J. Wong-ekkabut and M. Karttunen, *Biochim. Biophys. Acta*, 2016, **1858**, 2529.
44 W. Humphrey, A. Dalke and K. Schulten, *J. Mol. Graphics*, 1996, **14**, 33–38.
45 G. M. Torrie and J. P. Valleau, *J. Comput. Phys.*, 1977, **23**, 187–199.
46 S. Kumar, J. M. Rosenberg, D. Bouzida, R. H. Swendsen, P. A. Kollman and J. M. Rosenbergl, *J. Comput. Chem.*, 1992, **13**, 1011–1021.
47 J. S. Hub, F. K. Winkler, M. Merrick and B. L. de Groot, *J. Am. Chem. Soc.*, 2010, **132**, 13251–13263.
48 W. F. D. Bennett, J. L. MacCallum, M. J. Hinner, S. J. Marrink and D. P. Tieleman, *J. Am. Chem. Soc.*, 2009, **131**, 12714–12720.
49 J. Van der Paal, E. C. Neyts, C. C. W. Verlackt and A. Bogaerts, *Chem. Sci.*, 2016, **7**, 489–498.
50 C. Hofsass, E. Lindahl and O. Edholm, *Biophys. J.*, 2003, **84**, 2192–2206.
51 B. B. Issack and G. H. Peslherbe, *J. Phys. Chem. B*, 2015, **119**, 9391–9400.
52 H. Saito and W. Shinoda, *J. Phys. Chem. B*, 2011, **115**, 15241–15250.
53 J. M. Tucker and D. M. Townsend, *Biomed. Pharmacother.*, 2005, **59**, 380–387.
54 A. Azzi, R. Gysin, P. Kempna, R. Ricciarelli, L. Villacorta, T. Visarius and J. M. Zingg, *Mol. Aspects Med.*, 2003, **24**, 325–336.
55 Institute of Medicine, Vitamin E, Dietary Reference Intakes for Vitamin C, Vitamin E, Selenium, and Carotenoids, The National Academies Press, Washington, DC, 2000.
56 F. H. Lin, J. Y. Lin, R. D. Gupta, J. A. Tournas, J. A. Burch, M. A. Selim, N. A. Monteiro-Riviere, J. M. Grichnik, J. Zielinski and S. R. Pinnell, *J. Invest. Dermatol.*, 2005, **125**, 826–832.
57 J. Krutmann, *Hautarzt*, 2011, **62**, 576.

